IEEE Access
Multidisciplinary ⋮ Rapid Review ⋮ Open Access Journal

Received December 15, 2020, accepted December 23, 2020, date of publication December 30, 2020,
date of current version January 11, 2021.

Digital Object Identifier 10.1109/ACCESS.2020.3047885

A Permissioned Blockchain System to Reduce Peak Demand in Residential Communities via Energy Trading: A Real-World Case Study

SHIVAM SAXENA[1], (Student Member, IEEE), HANY E. Z. FARAG[1], (Senior Member, IEEE), AIDAN BROOKSON[2], HJALMAR TURESSON[3], AND HENRY KIM[3]

[1]Department of Electrical Engineering and Computer Science, York University, Toronto, ON M3J 1P3, Canada
[2]Sustainable Technologies Evaluation Program, Toronto and Region Conservation Authority, Toronto, ON L4K 5R6, Canada
[3]Schulich School of Business and Management, York University, Toronto, ON M3J 1P3, Canada

Corresponding author: Shivam Saxena (shivam@yorku.ca)

The authors are grateful to the MEARIE Group and Natural Resources Canada for providing funding and logistical support for this work.

ABSTRACT Residential energy trading systems (RETS) enable homeowners with distributed energy resources (DERs) to participate in virtualized energy markets that have the potential to reduce the peak demand of residential communities. Blockchains are key enablers of RETS, by virtue of providing a decentralized, self-governed network that mitigates concerns regarding privacy and transparency. However, more real-world case studies are needed to evaluate the techno-economic viability of blockchain-based RETS to improve their positive uptake. Thus, this article develops a permissioned blockchain-based RETS, which enables homeowners to select bidding strategies that consider the individual preferences of their DERs, and further evaluates the impact of the bidding strategies on reducing the peak demand of the community. The proposed system is implemented on the permissioned Hyperledger Fabric platform, where a decentralized ledger is used to store all energy bids, and a smart contract is used to execute a double auction mechanism and dispatch the homeowner DERs. The proposed system is validated by conducting simulations on a 8-home community using real-world data, and also by deploying the system to a Canadian microgrid, where the smart contract execution time is benchmarked. Simulation results demonstrate the efficacy of the proposed system by achieving a peak demand reduction of up to 48 kW (62%), which leads to an average savings of $1.02 M for the distribution system operator by avoiding transformer upgrades. Also, the simulation results show that the execution time of the proposed smart contract is 17.12 seconds across 12 nodes, which is sufficient for RETS.

INDEX TERMS Blockchain, energy trading, microgrid, distributed energy resources, smart contract, smart home, transactive energy.

I. INTRODUCTION

The proliferation of distributed energy resources (DERs) within residential communities, such as rooftop photovoltaic arrays (PV), plug-in electric vehicles (EV), smart thermostats (ST), and battery energy storage systems (BESS), is primarily motivated by homeowners seeking to reduce their energy costs [1]. Additionally, homeowners are seeking to increase their energy flexibility by having the option to rapidly switch between energy service providers that offer customized tariff structures, which consider homeowner preferences that seek to maximize the use of renewable resources [2]. Given the complexity of these customized tariff structures, homeowners also require transparent and automated energy billing that would remove inconsistencies in the recorded energy consumption and guarantee that the source of energy is from a verifiable renewable source [3].

In order to satisfy the aforementioned requirements, home energy management systems (HEMS) are typically proposed, where homeowners specify energy preferences related to the operation of their DERs, and the HEMS generates a dispatch schedule for the DERs as a result [4]. Thus, the presence of a HEMS transforms a home into a *smart home*, which is capable of autonomously controlling the DERs of the homeowner to achieve energy savings. However, a significant limitation of HEMS' is that they typically provide local

The associate editor coordinating the review of this manuscript and approving it for publication was Yonghao Gui.

control of a single home, and they do not have observability of the entire residential community [5]. This leads to uncoordinated operation of DERs within the community, which may result in major increases in peak demand and overloading of transformers when EVs and BESSs are charging coincidentally [6]. Thus, new mechanisms are needed to facilitate the coordination of DERs at the community level, while also taking the local transformer capacity into account. Since this scenario involves the presence of homeowners and the distribution system operator (DSO), each with potentially conflicting objectives, the mechanism must provide a framework that enables trust, transparency, and impartiality [7].

A promising mechanism that satisfies these requirements is peer to peer (P2P) residential energy trading systems (RETS), where homeowners, analogous to peers, can utilize their DERs to trade energy within their community at their discretion [8]. The trading is supported by a virtual energy marketplace, which divides the day into discrete market intervals, wherein homeowners submit bids for each DER and a market clearing process is executed by an auctioneer to determine if the bid is granted [9]. DSOs may also participate in the marketplace by setting maximum limits for the available demand allowed within the market interval. Recently, blockchain technology has been proposed as a key facilitator of RETS because of its ability to provide a decentralized, transparent ledger of transactions that could mitigate trust issues between peers such as homeowners and DSOs [10]. Each transaction is first encrypted to prevent unauthorized parties from reading transaction details, verified by peers using a consensus mechanism, and then collected into discrete blocks that are appended to the ledger in tamper-proof fashion [11]. Blockchains are further empowered by automated smart contracts, which are used to initiate and verify transactions between peers. Thus, blockchains can further enable RETS because they i) obviate the need for an auctioneer and allow homeowners and DSOs to engage on impartial terms; ii) protect the privacy of homeowner transactions using encryption techniques; and iii) facilitate transparent billing practices that establish the provenance of all energy transactions on the ledger [3].

Blockchain-based RETS is a recent topic of great interest [12]–[26], where strong contributions have been made by prior works with respect to criteria such as the consideration of homeowner bidding strategies, evaluation of financial savings, benchmarking evaluation of scalability, as well as the evidence of real-world implementation. A comparative table that summarizes the prior works with respect to the aforementioned criteria can be found in Table 1.

The works in [12]–[15] develop bidding strategies for homeowners that consider their preferences for the operational use of their DERs, which are typically time-varying [27], [28]. The authors in [12] and [13] propose a permissioned blockchain system that utilizes contract theory to model the preference of EV owners to prioritize energy trading with solar energy aggregators, where smart contracts are used to audit all energy transactions. The authors in [14] and [15] focus on evaluating the preferences of different classes of users to interrupt the schedules of their general appliances and DERs at strategic times to increase energy savings. However, the papers in [12]–[15] do not model bidding strategies for BESSs or STs, and thus, they do not accurately represent the complete range of DERs that would be able to participate in RETS [27].

TABLE 1. Comparison Table of Related Work With Proposed Work

Reference	Criteria #1: Bidding Strategies	Criteria #2: Financial Evaluation?	Criteria #3 Bench-marking?	Criteria #4: Real-world Deployment
[12]	✓			
[13]	✓	✓		
[14], [15]	✓	✓		
[16]–[19]		✓		
[20], [21]			✓	
[22]	✓		✓	
[23]		✓	✓	
[24]–[26]			✓	
Proposed paper	✓	✓	✓	✓

The works in [16]–[19] focus on evaluating the financial feasibility of blockchain-based RETS. In [17], a RETS is proposed to facilitate trades between homeowners and a community BESS, which leads to monthly savings of $75.92 (44.2%). In [18], a game-theory based system is developed to enable homeowners to form coalitions and negotiate electricity rates that lead to monthly savings of $378.2 across 300 homeowners. The authors in [19] implement an Ethereum-based smart contract, based on non-cooperative game theory, to generate daily savings of 24 Chinese Yen (CNY) across 6 households equipped with PV and interruptible loads. The work in [16] develops an energy trading algorithm that minimizes the number of transactions on the ledger to reduce communication overhead. Yet, the aforementioned works do not discuss the financial impact on the presiding DSO, which leaves the financial analysis incomplete.

The works in [20]–[26] focus on benchmarking the scalability of their blockchain-based systems. In [20], an Ethereum-based smart contract is developed, which can execute 100 trades per market interval at an average transaction latency of 42.6 seconds. The authors in [21] propose a partial-permission based consensus algorithm that reduces the energy trading time by 57.2% when compared to the Proof of Work (PoW) mechanism. In [22], the impact of providing enhanced privacy protection within Ethereum-based smart contracts is evaluated at an average transaction latency of 45 seconds per 1000 transactions. The work in [23] benchmarks the total computation time between two nodes within an private Ethereum-based system, which is measured at 33 milliseconds. The authors in [24] develop an innovative on-chain storage technique that reduces the cost of storage for energy trading transactions by 125%. In [25], energy trading algorithms are developed to optimize blockchain-based storage costs and energy transfer costs. The authors in [26] develop a fog-based blockchain system architecture for

energy trading within smart cities, where the average transaction latency is 3 seconds. However, the aforementioned works restrict the benchmarking evaluation to public or private blockchain platforms architectures, and do not consider permissioned blockchain architectures, such as Hyperledger Fabric (HLF), which could provide greater scalability [29].

It is worth mentioning that while none of the aforementioned works have deployed their systems within a real-world environment with physical DERs, several real-world pilots have been launched by companies such as Drift and Restart Energy for this purpose [30]. Both companies offer blockchain-based systems to enable homeowners to specify the source of energy they require, while projecting energy savings of 20%. However, to the best of the authors knowledge, benchmarking evaluations of their proposed systems have not been published.

To those ends, this article proposes a permissioned blockchain implementation for a RETS that enables the reduction of peak demand within a community. A permissioned blockchain architecture is chosen because it requires only a subset of qualified peers to participate in the consensus process, leading to lower transaction latency [31]. A smart contract is developed to administer the RETS by validating all energy bids within a market interval, finding the market clearing price (MCP) via the double auction method, and dispatching the MCPs appropriately. Bidding strategies for EVs, STs, and BESSs are explicitly modeled based on homeowner preferences that characterize how DERs can be either ''helpful'' or ''selfish'', which reflect the willingness of the homeowner to alter the operational schedule of their DERs to reduce peak demand. Since BESSs are the only bi-directional DER in this work, a fuzzy logic-based bidding strategy is proposed to handle this additional complexity, which considers parameters such as the time of day, net load, and state of charge (SoC). The proposed system also enables DSOs to set demand caps on the community to limit the allowable peak demand. Simulated experiments are executed to demonstrate the proposed system's ability to reduce peak demand when the market is dominated by helpful BESSs, as well as when DSOs place demand caps on the community. The results of the simulated experiments further inform a financial assessment on five large DSOs in Ontario, Canada, which quantifies the average capital expenditure (CAPEX) savings for the DSOs by avoiding upgrades to transformer capacity as a result of the reduction in peak demand. Lastly, the proposed system is implemented on the permissioned HLF platform and deployed to a real-world Canadian microgrid, where the execution time of the proposed smart contract is benchmarked across 12 nodes, and its ability to reduce demand and minimize energy imports from the DSO is highlighted.

Specifically addressing the technical gaps identified in the aforementioned prior works, the key contributions of this article are summarized as follows: i) development of novel homeowner bidding strategies for BESSs, EVs, and STs that characterize helpful or selfish behavior; ii) financial evaluation of the CAPEX savings generated by the proposed system for DSOs; iii) benchmarking of the smart contract execution time on the permissioned HLF platform, and iv) real-world deployment of the proposed system at a Canadian microgrid.

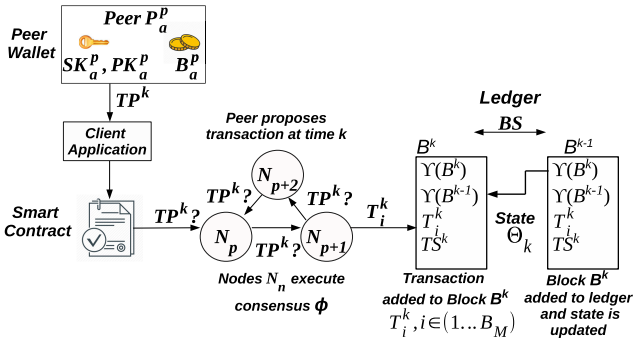

FIGURE 1. A generalized representation of a blockchain network.

The organization for the remainder of the article is as follows. Section II provides a review of blockchain technology, Section III introduces the modeling of the smart home DERs and residential communities. Section IV introduces the proposed bidding strategies for STs, EVs, and BESSs. Section V covers the design of the permissioned blockchain architecture for the proposed system, while Section VI presents the results of the simulated and real-world experiments. Finally, Section VII is reserved for conclusions and future work.

II. REVIEW OF BLOCKCHAIN TECHNOLOGY

The goal of any blockchain system is to ensure that the system state is consistently agreed upon by the peers in the network, where the system state is composed of the P2P transactions that are stored on the ledger [11]. Figure 1 shows a symbolic representation of a general blockchain network, which depicts the process of how transactions are committed to the ledger. Each peer, P, utilizes a computing resource, referred to as a node, N, to interface with the blockchain network. Multiple peers can be assigned to a single node [32], and thus, a peer can be denoted as P_a^p, where a is the index of the peer assigned to the node ID, p. Upon joining the blockchain network, the peer receives a digital wallet that stores its account balance, B_a^p, as well as its public/private keys, $\{SK_a^p, PK_a^p\}$, that are used to sign each transaction to establish the identity of the transaction owner. Transactions are made by the peer by invoking a smart contract, which is a set of automated functions that are deployed on the ledger and are accessed by the peer via a client application [33].

Before the transaction is stored on the ledger, however, the transaction must be validated by the peers using a consensus mechanism, where popular consensus mechanisms include PoW and practical byzantine fault tolerance (pBFT) [34]. As depicted in Figure 1, a peer initiates the consensus mechanism, ϕ, at time k by generating a transaction proposal, TP^k. Subsequently, TP^k is forwarded to other nodes that individually verify the validity of the transaction according to rules that are determined within the smart

contract [35]. If a minimum of two-thirds of the nodes report that TP^k is indeed valid, it is added to a block of transactions, B^k, which stores the transaction into the block as an ordered set, T_i^k, $i \in (1 \dots B_M)$, where i is the index of the transaction and B_M is the maximum block size. The block also contains a timestamp, TS^k, as well as a block hash, $\Upsilon(B^k)$, that is uniquely composed of all the transactions within the block, and is updated with every new transaction. A new block is created when the block has reached its maximum block size, or, when a certain amount of time has elapsed since the last block was created, referred to as the block speed, BS. The new block is appended to the end of the ledger and pointed at the block hash of the previous block, $\Upsilon(B^{k-1})$, resulting in ledger data that is transparent and tamper-proof. Thus, the current state of the blockchain, denoted as Θ_k, is a reflection of the transactions of the latest block on the ledger after having been verified by ϕ, as well as the blocks that came before it, and can be formulated as:

$$\Theta_k = \phi(B^k, B^{k-1}, B^{k-2} \dots B^0) \tag{1}$$

It is important to note, however, that the time taken to reach consensus for each transaction is not equal [36], and therefore, benchmarks are required to evaluate the execution time of blockchain-based energy trading systems, as will be seen in Section V.C.

III. MODELING OF DERs WITHIN A SMART HOME

This section introduces the mathematical modeling of DERs within a smart home, including BESSs, EVs, PVs, and STs, as well as the derivation of the total peak demand of a community and potential CAPEX required by the DSO to support it. To provide real-world context, the main concern of DSOs with respect to DERs owned by homeowners is that their operational schedules are usually left uncontrolled [37]. As such, the typical behavior of a homeowner possessing a DER would be to increase its consumption during the time of day when electricity is inexpensive, leading to scenarios where the peak demand of the community can exceed the capacity of the local transformer [38]. As such, it is important to formulate models that describe the operation of the aforementioned DERs such that baseline load profiles for a community of smart homes can be generated, and the maximum peak demand of the community can be quantified. Thus, the rest of the section will provide the mathematical models of the DERs. In general, a set of smart homes, denoted by subscript m, possess any combination of DERs, denoted by subscript n, where the variable k signifies discrete time.

A. MODELING OF BESSs AND EVs

A BESS is modeled as a bi-directional DER, where the power output of the BESS ($P_{BESS,m,n}$) is constrained by the maximum and minimum limits of its onboard inverter, and the SoC of the BESS ($SoC_{BESS,m,n}$) should remain within the recommended limit of the manufacturer. The aforementioned constraints can be seen in (2)-(3), while the equation for the SoC of the BESS is derived in (4).

$$P^{MIN}_{BESS,m,n} \leq P_{BESS,m,n}(k) \leq P^{MAX}_{BESS,m,n} \tag{2}$$

$$SoC^{MIN}_{BESS,m,n} \leq SoC_{BESS,m,n}(k) \leq SoC^{MAX}_{BESS,m,n} \tag{3}$$

$$\begin{aligned} SoC_{BESS,m,n}(k) = {} & SoC_{BESS,m,n}(k-1) \\ & + \left(\chi_{m,n} \cdot \eta^{CH}_{m,n} - (1-\chi_{m,n})\eta^{DIS}_{m,n}\right) \\ & \times P_{BESS,m,n}(k-1) \end{aligned} \tag{4}$$

where, $\{P^{MIN}_{BESS}, P^{MAX}_{BESS}\}$ are the minimum and maximum power limits, $P_{BESS}(k)$ is the instantaneous power requirement, $\{SoC^{MIN}_{BESS}, SoC^{MAX}_{BESS}\}$ are the minimum and maximum SoC limits, $SoC_{BESS}(k)$ is the current SoC, χ is a binary variable that represents 1 for charging mode and 0 otherwise, and $\{\eta^{CH}, \eta^{DIS}\}$ are the charging and discharging efficiencies, respectively.

On the other hand, an EV is modeled as a unidirectional load, as seen in (5).

$$\begin{aligned} SoC_{EV,m,n}(k) = {} & SoC_{EV,m,n}(k-1) \\ & + \left(\chi_{m,n} \cdot \eta^{CH}_{m,n}\right) P_{EV,m,n}(k-1) \end{aligned} \tag{5}$$

The EV is subject to the same constraints as in (2)-(3), in addition to a constraint that specifies that the SoC of the EV should be greater or equal than a desired level of SoC before a target departure time, as seen in (6). Generally, this constraint forces a homeowner to charge the EV to a minimum amount before the departure time to ensure that the EV has enough SoC for its trip [39].

$$SoC_{EV,m,n}(k_{Dep}) \geq SoC^{Des}_{EV,m,n}(k_{Dep}) \tag{6}$$

where k_{Dep} is the time of departure for an EV, $SoC_{EV}(k_{Dep})$ is the SoC at the time of departure, and $SoC^{Des}_{EV}(k_{Dep})$ is the desired SoC to be reached before the time of departure. It is worth noting that the modeling for the discharging of the EV is not covered within this article, where the modeling is a function of the daily driving distance of the vehicle (in kilometers - km) and the energy consumption per distance traveled (kWh/km) [40]. As in [40], we assume that the SoC of the EV depletes at a linear rate throughout the day, and begins to charge when it arrives at home.

B. MODELING OF PVs

The direct current (DC) power generated from a PV array can be found as follows [41],

$$P^{DC}_{PV,m,n} = P^{RT}_{PV,m,n} IRR(k) F_T(T_{m,n})(k) \tag{7}$$

where, P^{DC}_{PV} is the DC power generated by the PV array, P^{RT}_{PV} is the nameplate rating of the PV array, IRR is the current level of irradiance in kW/m^2, T is the current temperature in °C, and F_T is an interpolated temperature factor that can be found in [41]. The alternating current (AC) power output of the PV system can then be found as follows,

$$P_{PV,m,n}(k) = P^{DC}_{PV,m,n}(k) \psi_{m,n} \tag{8}$$

where, $P_{PV,m,n}$ is the final AC output power of the PV system, and $\psi_{m,n}$ is the inverter efficiency that can be interpolated using methods and data found in [41].

C. MODELING OF STs

The modeling of the ST depends on the dynamics of the indoor temperature of the home, which is presented below [42].

$$T_{in,m}(k) = T_{in,m}(k-1) + \beta\Delta k\Big(P_{ST,m}(k-1) - \lambda(T_{in,m}(k-1) - T_{out,m}(k-1))\Big) \quad (9)$$

where T_{in} is the indoor temperature (°C), Δk is the period of time between timesteps k and $k-1$, β is the inverse of the heat capacity (°C/Joules), P_{ST} is the heating power of the ST (kW), λ is the heat loss coefficient (kW/°C), and T_{out} is the outdoor temperature (°C). The equation describing the energy consumption of the ST (E_{ST}) as a function of the indoor, outdoor, and setpoint temperatures ($T_{set,m}$) is [43]:

$$\beta E_{ST,m}(k) = \lambda\beta\Delta k T_{out,m}(k) - T_{set,m}(k) - (\lambda\beta\Delta k - 1)T_{in,m}(k) \quad (10)$$

Rearranging, the energy consumption of the ST of a home can be formulated as:

$$E_{ST,m}(k) = \lambda\Delta k T_{out,m}(k) - T_{set,m}(k)/\beta - (\lambda\Delta k - 1/\beta)T_{in,m}(k) \quad (11)$$

D. COMMUNITY MODELING

In general, a residential community, denoted by subscript i, is composed of a number of smart homes (N_m) and associated DERs (N_n). Thus, the peak demand of any single community, i, can be represented as:

$$P_{PEAK,i}(k) = \max_{\forall k \in P}\left(\sum_{a=1}^{N_m}\sum_{b=1}^{N_n} P_{DER,m,n}(k) + L_m(k)\right) \quad (12)$$

where, P is a set of k time indexes that represent a period of time, $P_{DER,m,n}$ is the generalized form of any of the aforementioned DERs, and L_m represents critical house loads that are uninterruptible, such as lighting and appliances. To avoid overloading the local transformer that serves the community, $P_{PEAK,i}$ must be less than the transformer capacity, denoted by $T_{CAP,i}$. If $P_{PEAK,i}$ exceeds $T_{CAP,i}$, the presiding DSO most invest in CAPEX to replace or upgrade $T_{CAP,i}$ as seen in the following equation,

$$CAPEX_i = \begin{cases} PT^{NEW}_{CAP,i} - PT^{OLD}_{CAP,i}, & P_{PEAK,i} > T_{CAP,i} \\ PT^{OLD}_{CAP,i}, & P_{PEAK,i} < T_{CAP,i} \end{cases} \quad (13)$$

where, PT^{NEW}_{CAP} is the price of the new transformer with upgraded capacity, and PT^{OLD}_{CAP} is the price of a transformer with the same capacity. The CAPEX calculation assumes that the transformer will be replaced at one point during its lifetime. Thus, if $P_{PEAK,i}$ does not exceed $T_{CAP,i}$, the DSO will still bear the cost of a single replacement, but will save the cost of upgrading its capacity.

Thus, the specific problem that the proposed system seeks to mitigate is to reduce the peak demand of a community by facilitating a RETS, whereby homeowners may elect to bid and trade energy during discrete intervals of the day. Each homeowner may have different strategies that would affect the price and quantity of the bid per DER, and the ability of the proposed system to utilize these bidding strategies to reduce the peak demand of the community is a key contribution of the proposed article. The metrics used to evaluate the viability of the proposed system will be the total reduction of peak demand within the community (kW), as well as the total CAPEX savings realized by avoiding capacity upgrades to local transformers as a result of the reduction (measured in $ CAD).

IV. PROPOSED HOMEOWNER BIDDING STRATEGIES

This section introduces the proposed bidding strategies for homeowners in context of their participation in a residential community marketplace. In this article, bidding strategies are defined only for the controllable DERs, which are STs, BESSs, and EVs, while PVs are assumed to have static bids.

A. OVERVIEW OF RESIDENTIAL COMMUNITY ENERGY MARKETPLACES

A common method used to calculate the MCP of electricity markets is the double auction method [44]. In a double auction, an auctioneer receives energy bids from market participants for each discrete market interval during the day, where an energy bid is represented by a corresponding quantity and price. The auctioneer first divides the bids into generation and load bids, and then sorts the generation bids by ascending price and the load bids by descending price, thus generating a supply curve and a demand curve, respectively. The intersection between the two curves is computed as the MCP of the market interval, where only bid prices lower than the MCP are granted. The implementation of the double auction method results in the merit-order effect, where the most expensive load bids are satisfied by the most inexpensive generation bids [39].

Figure 2 shows the double auction method that is adapted for a community marketplace, where generator bids can be submitted by PVs or BESSs, while load bids can be submitted by BESSs, STs, and EVs. As discussed earlier, critical loads are those house loads that cannot be interrupted, and thus, they are slotted at the highest price on the load curve. The presiding DSO is able to submit energy bids during the market interval, referred to as grid bids, and is also able to set a demand cap that limits the total community demand within the interval. As seen in Figure 2, a potential scenario has the demand cap placed at a vertical bid of 0.6 kWh with a corresponding price that tends towards infinity, which results in an MCP of $0.13/kWh (MCP 1), and further results in only the critical bids being granted. As more DER penetration enters the market, the merit-order effect occurs, and more load bids are granted as a result of the MCP being lowered, as seen by MCP 2 ($0.12/kWh) and MCP 3 ($0.07/kWh).

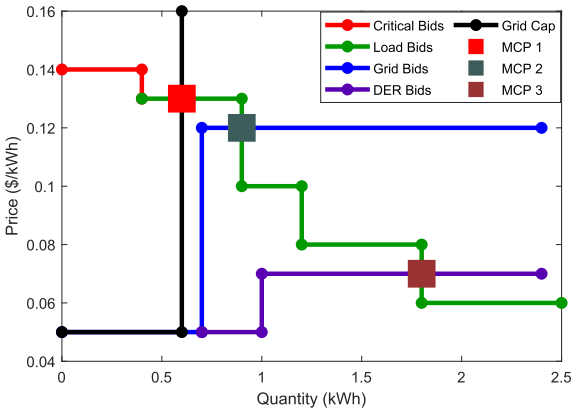

FIGURE 2. Community marketplace representation.

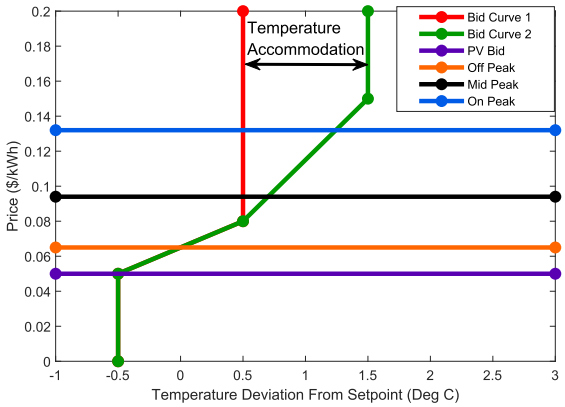

FIGURE 3. Example bid curves of STs.

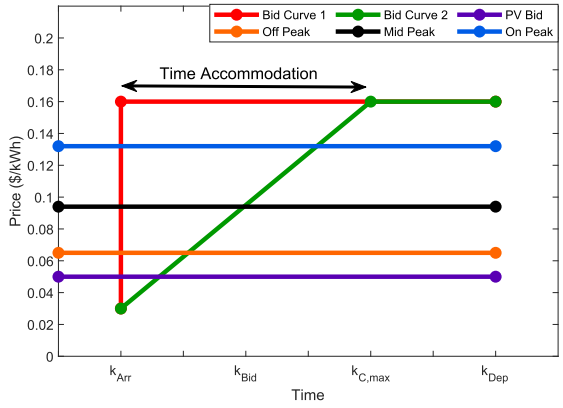

FIGURE 4. Example bid curves of EVs.

B. BIDDING STRATEGIES FOR STs AND EVs

Since a bidding curve represents a collection of energy bids that map the bid's energy quantity to a price that a homeowner is willing to pay for that quantity, a homeowner may face difficulty in determining precise values for their bid curve. Thus, the bidding curves proposed in this article aim to provide an intuitive, indirect method of mapping the bid quantity to the bid price by reflecting the bid quantity as a function of the DER's operational attributes. Consequently, the bid curve reflects the willingness of a homeowner to alter their DER's operational schedule, thereby adjusting its bid quantity, based on the *value* of the service it provides [39]. In the case of STs, the item of value is the flexibility of thermal comfort, and in the case of EVs, the item of value is the flexibility of reaching the desired SoC before a target departure time [7]. Each point along these bid curves indirectly reflects the quantity of energy required by the DER at a price point that the homeowner is willing to pay for it, thus aligning with the bid curve depicted in Figure 2. Thus, this article considers the formulation of *selfish* and *helpful* bidding strategies, where helpful homeowners are much more willing to disrupt a DER's operating schedule in comparison to selfish homeowners. As a result, helpful DER owners generate more flexible bid curves than selfish DER owners, and therefore, helpful DER bid curves tend to have greater potential in reducing peak demand. It is worth mentioning that the classification of bidding strategies as selfish and helpful have been used widely, as in [45] and [46].

For instance, Figure 3 depicts two separate bidding curves for STs, where the bid curves symbolize the incremental price a ST is willing to pay as a function of thermal discomfort, which can be measured by the temperature deviation from its desired setpoint [7]. Also depicted in Figure 3 are generation bids that follow the electricity pricing defined by typical time of use (TOU) rate plans offered by DSOs [47], where higher rates are charged during on-peak and mid-peak hours, and lower rates are charged at the off-peak hours. A sample bid of PV energy is also shown in Figure 3. Thus, the intersection of the ST bid curve with each of the generation bids represents the price that the ST is willing to pay per unit of temperature deviation from the setpoint, per provider of energy. As such, Bid Curve 1 can tolerate a maximum temperature deviation of $+0.5$ °C, from which point, the vertical line at $+0.5$ °C signifies that the ST will pay *any* price for its bid to be accepted and for thermal comfort to be restored. On the other hand, Bid Curve 2 has much more flexibility, since it can tolerate a maximum temperature deviation of $+1.5$ °C. The difference in maximum acceptable temperature deviation between Bid Curve 1 and Bid Curve 2 is representative of how much more accommodating, or helpful, Bid Curve 2 can be in reducing peak demand. Thus, Bid Curve 2 is characterized as being more helpful than Bid Curve 1.

Similarly, bidding curves for EVs are depicted in Figure 4, where k_{Arr} is the arrival time of the EV, k_{Bid} is the time when the homeowner makes a bid for the EV, $k_{C,max}$ is the maximum time the EV can wait before it must charge at full power to reach a desired SoC based on the time of departure, and k_{Dep} is the time of departure of the EV. As seen in Figure 4, the vertical line of Bid Curve 1 at k_{Arr} indicates that at the time of arrival, the EV is willing to pay any electricity price to start charging, and that there is absolutely no flexibility or time accommodation it considers in its bidding strategy. On the other hand, Bid Curve 2 is more flexible, and is willing to bid in the market by steadily increasing its bid price until $k_{C,max}$. At this point, the two bid curves converge, thus representing that the EVs would need maximum charging power to reach

the desired SoC before k_{Dep}. Thus, it follows that the Bid Curve 2 is more helpful than Bid Curve 1 because of its willingness to provide more accommodation in terms of time.

As such, it follows that the lack of flexibility for selfish DERs inhibit their ability to participate in initiatives to reduce the peak demand of the community, as will be demonstrated in the simulation results.

C. FUZZY BIDDING STRATEGY FOR BESSs

As shown in Figures 3 and 4, the bidding curve for the STs and EVs can be formulated by a single input and a single output. However, the BESS is bi-directional in nature, and its bidding strategy must accommodate a wider range of input parameters, such as the need to retain enough SoC to provide power to critical house loads, while also being watchful of market prices to reduce its operating cost. The addition of complex input parameters requires precise numerical limits to be in place to generate a bidding curve for the BESS, which can be difficult to obtain [48]. Alternatively, fuzzy logic can be used to classify the input parameters into a set of imprecise variables, which are then evaluated against plain-language rules to generate specific outputs. The classification process involves the usage of a fuzzy membership function, which specifies the degree by which an input/output parameter belongs to specific variable, and is quantified between the range of 0 (no membership) to 1 (full membership). Since the membership function allows partial membership, the input parameters can be easily tuned, and thus, fuzzy logic is a viable option to overcome uncertainty in defining precise limits within a system [48].

As such, a fuzzy bidding strategy is proposed for BESSs in this article, where the block diagram of the bidding strategy can be seen in Figure 5. The proposed fuzzy bidding strategy has three discrete inputs, which are the time of day, the net load of the house, as well as SoC of the BESS. These discrete input variables are then fuzzified to their corresponding fuzzy variables using input membership functions, which are depicted in Figure 6. For the net load, the membership function defines three fuzzy variables, which are surplus (generation of home exceeds demand), deficit (demand exceeds generation), and neutral (minimal level of surplus or deficit). For the BESS SoC, the membership function also defines three fuzzy variables, which are low, medium, and high. The shape of these two membership functions are triangular, which reflect the degree of membership by which the discrete input variable belongs to the fuzzy variables. It is worthwhile to mention that the membership function for the time of day is not depicted because there is no uncertainty as to when the off/mid/on peak times are, and thus, the resultant membership function is simply binary.

After the fuzzification process classifies the input parameters into a set of fuzzy variables, the fuzzy rule set evaluates the variables and generates a set of fuzzy outputs. The fuzzy rule set depicted in Figure 5 aligns with the earlier mentioned methodology of classifying homeowners as selfish and helpful. In this case, a selfish BESS is motivated by financial opportunity, thereby charging at off-peak periods when the market price tends to be lower, and discharging at on-peak periods to gain maximum revenue. On the other hand, a helpful BESS is motivated by self-consumption, charging only when there is excess PV energy available during the day, and discharging during the evening off-peak period when other DERs would be drawing power to take advantage of off-peak prices. The aforementioned description of the strategies is reflected by the fuzzy rule set, where the helpful BESS seeks to charge when the net load of its home is not at a deficit or when there are off-peak periods, and will

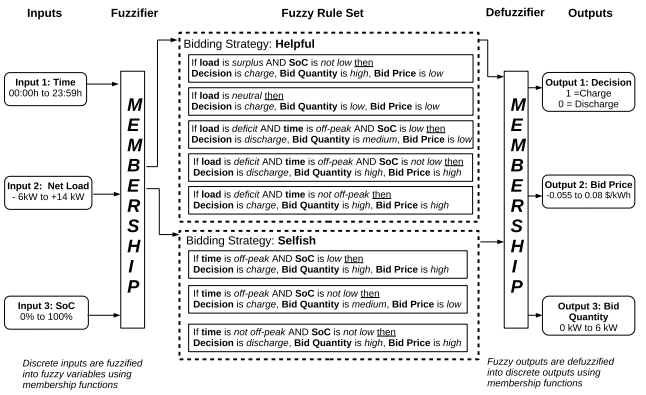

FIGURE 5. Block diagram of proposed fuzzy logic-based BESS bidding strategy.

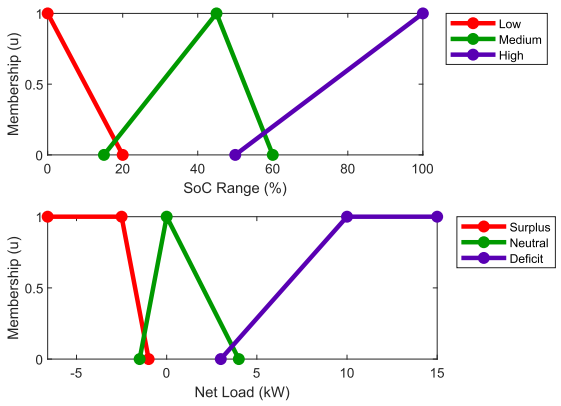

FIGURE 6. Input fuzzy membership functions.

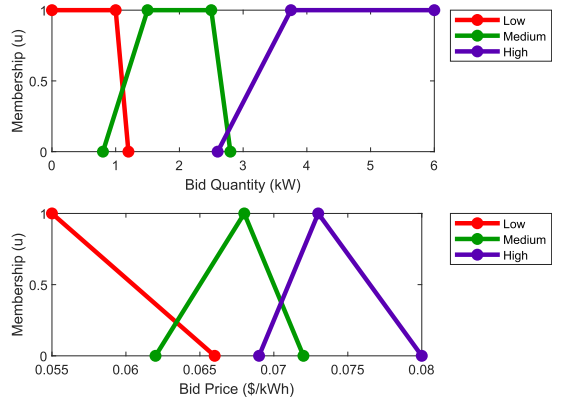

FIGURE 7. Output fuzzy membership functions.

vary the quantity of its bid depending on the net load. The strategy attempts to ensure that the BESS retains enough SoC throughout the day such that it can discharge in the evening off-peak period. On the other hand, the selfish BESS always discharges in off-peak periods as long as its SoC is not low, while keeping the bid price and bid quantity high to maximize revenue.

Once the fuzzy rule set evaluates the input fuzzy variables, it generates output fuzzy variables that must be defuzzified into discrete outputs using output membership functions. These discrete outputs are the charging decision, the bid price, and the bid quantity. The output membership functions that describe these variables can be seen in Figure 7. The charging decision variable has binary outputs, which are either to charge (1) or discharge (0), while on the other hand, both the bid price and bid quantity define variables of low, medium, and high. Combined together, these discrete outputs completely describe the bidding strategy of the BESS with numerical values of what the bid price and quantity should be for a specific time interval during the day. It is worthwhile to mention that the membership functions seen in Figures 6 and 7 were tuned using trial and error methods with the objective of finding the best possible configuration to maximize the reduction of peak demand, as will be seen in the experimental results presented in Section VI.

V. DESIGN OF PERMISSIONED BLOCKCHAIN SYSTEM

The proposed system is developed using HLF, which is a permissioned blockchain development platform that enables the peers within a blockchain network to be segregated into private channels [7]. Each channel is assigned a separate ledger and smart contracts, where the data on the ledger is kept hidden from other channels, thus leading to increased data privacy for the peers [49]. In this article, each community is designated its own channel, as can be seen in the architectural block diagram of the proposed system in Figure 8. The ledger stores three items, including data structures that represent a market interval, bids, and DER measurements. The market interval is represented by an interval ID, denoted by M_{ID}, the MCP for the interval, symbolized by MCP_{ID}, and the interval time expiry, denoted by TXP^{k}_{ID}. The bids, denoted as BID^{p}_{a}, are indexed according to the M_{ID}, where the $^{p}_{a}$ notation represents the identity of the homeowner. Each bid has a corresponding bid price and quantity, which are denoted as $\{PR^{p}_{a}, Q^{p}_{a}\}$, respectively, and are associated with a DER, symbolized by $DER_{m,n}$. Each bid also has a unique timestamp, denoted by TS^{k}. Measurements from each DER are also stored to the ledger, denoted by E^{p}_{a}, along with the corresponding market interval, DER, and timestamp. The smart contract provides functions that autonomously administer the marketplace, including homeowner account initialization, creating a new market interval, submitting bids/measurements, as well as executing the double auction to find the MCP for the market interval. Also, the presiding DSO may submit generator bids, referred to as grid bids, or demand caps for each market interval, where the demand cap is

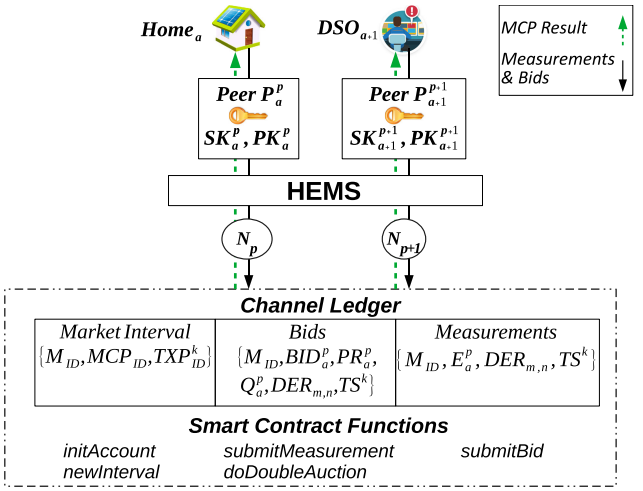

FIGURE 8. Architectural block diagram of proposed blockchain system.

denoted by G_{CAP}. It is assumed that homeowners interact with the proposed blockchain system via the user-interface of an HEMS.

In order to provide more clarity on the implementation of the smart contract, a description of each function is provided below. Additionally, the pseudo-code that describes every function of the smart contract is provided in Algorithm 1.

initAccount(): This function initializes an account for the homeowner by generating its public/private keys ($\{SK^{p}_{a}, PK^{p}_{a}\}$), and setting the account balance to zero (B^{p}_{a}).

newInterval(): This function creates a new M_{ID} at TS^{k}, initializes an empty list of bids ($[BID^{p}_{a}]$) for the M_{ID}, and assigns the time expiry for the M_{ID} after a fixed time interval (TXP^{k}_{ID}).

submitBid(): This function is called by homeowner P^{p}_{a}, which accepts inputs of M_{ID}, PR^{p}_{a}, Q^{p}_{a}, $DER_{m,n}$, and TS^{k}. The function validates the incoming bid by checking if i) the homeowner has sufficient B^{p}_{a} in their wallet to make a bid for PR^{p}_{a}, and ii) if the time of the bid TS^{k} has not exceeded the time expiry TXP^{k}_{ID}. If both conditions are true, the bid is added to list of bids within M_{ID}.

doDoubleAuction(): This function executes a double auction by sorting the bids into supply and demand curves, and applying G_{CAP} if supplied. Subsequently, the MCP_{ID} is computed by finding the intersection of the curves and is broadcasted to the HEMS, which actuates the DER in accordance to the MCP.

submitMeasurement(): This function stores an energy measurement, E^{p}_{a}, on the ledger, indexed by M_{ID}, $DER_{m,n}$ and TS^{k}.

Additionally, to clearly depict the workflow and demarcate the information exchanges between a homeowner, HEMS, and the proposed smart contract of the blockchain-based system, a sequence diagram is shown in Figure 9. After registering on the blockchain network and initializing an account (steps 1-2), the homeowner configures individual preferences for their DERs as discussed in Section IV. Then,

Algorithm 1 Proposed Smart Contract Implementation

function initAccount()
Input: Peer ID (P_a^p)
Generate SK_a^p, PK_a^p, initialize $B_a^p \leftarrow 0$
Output: $\{SK_a^p, PK_a^p, B_a^p\}$
function newInterval()
Create new market interval with time expiry, M_{ID} at TS^k
Create empty list on ledger to hold energy bids, $[BID_a^p]$
Output: $\{M_{ID}, TS^k, [BID_a^p]\}$
function submitBid()
Input: $\{M_{ID}, PR_a^p, Q_a^p, DER_{m,n}, TS^k\}$
Generate bid structure for BID_a^p based on inputs
if $PR_a^p \leq B_a^p$ && $TS^k \leq TXP_{ID}^k$
then append BID_a^p to list of bids $[BID_a^p]$
function doDoubleAuction()
Input: $\{M_{ID}, [BID_a^p], G_{CAP}\}$
Separate all bids into generation (G_{ID}) or load (L_{ID})
Sort G_{ID} by ascending price, L_{ID} by descending price
Apply G_{CAP} if supplied
Intersection of G_{ID} and $L_{ID} \rightarrow MCP_{ID}$.
Send notification to homeowner's HEMS for DER actuation.
Output: MCP_{ID}
function submitMeasurement()
Input: $\{M_{ID}, E_a^p, DER_{m,n}, TS^k\}$
Store E_a^p to ledger, indexed by $\{M_{ID}, DER_{m,n}, TS^k\}$

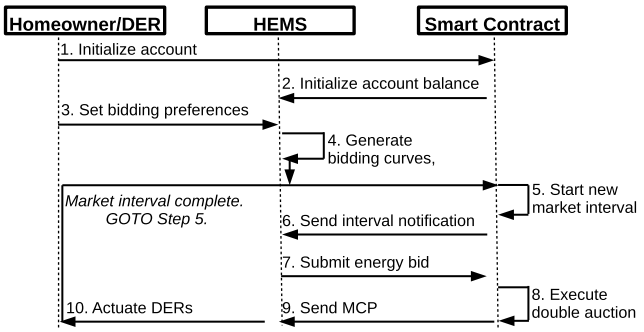

FIGURE 9. Sequence diagram of data flow across proposed system.

the HEMS uses the homeowner's preferences to generate bidding curves for the homeowner for each DER (steps 3-4). The smart contract then auto-creates a new market interval, and sends a notification to the HEMS to respond with a bid (steps 5-6). The smart contract collects valid energy bids from the HEMS, waits until the time expiry for the market interval has passed, calculates the MCP, and broadcasts the MCP back to the HEMS. The HEMS then actuates the DER of the homeowner according to the MCP (steps 7-10). That is, if the bid price is greater than the MCP, the DER is turned on and its power flow is regulated by the HEMS to the precise quantity of energy the DER bid for. Otherwise, the DER is turned off for the market interval. After the market interval closes, a new market interval is started after a configurable period of time, and steps 5-10 are repeated indefinitely.

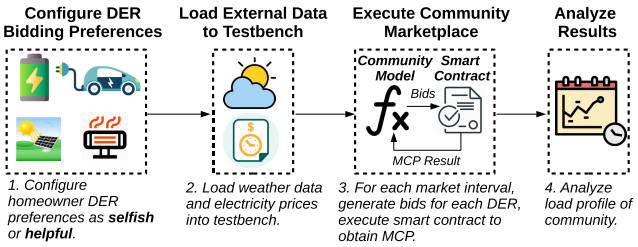

FIGURE 10. Workflow of testbench used to evaluate experimental results.

VI. EXPERIMENTAL RESULTS

This section presents the results of both simulated and real-world experiments. The simulated experiments are conducted on a testbench desktop application that is developed as a part of this work, where a workflow diagram of the testbench is depicted in Figure 10. First, the bidding preferences for each DER of each homeowner are configured as selfish or helpful. Second, weather data (indoor/outdoor temperature and irradiance) and electricity prices are separated into 5 minute market intervals and loaded into the testbench. Third, the load profile of the community is generated by equations (2)-(9) for every discrete market interval, and the bidding strategies for all DERs are then executed to generate bids for the market interval. The bids are evaluated by the proposed smart contract to generate the MCP for the market interval, and the MCP is fed back into the community model to determine the energy consumption/generation for each DER. When all market intervals have been evaluated, the testbench exports the resultant load profile of the community to a data file for further analysis.

Thus, the simulated experiments within this article involve a 8-home residential community, where each home is assumed to have a PV, BESS, EV, and ST. The nameplate ratings for these DERs are shown in Table 2. Real-world data collected over the period of 2016 from the Kortright Centre Microgrid (KCM) is used to generate the energy profile for each of the DERs, including the critical load of home appliances such as lighting, dishwashers, and refrigerators. With respect to the pricing of electricity, the on/off/mid peak periods are based on the Ontario 2016 TOU schedule, where off-peak periods are from 19:00 to 7:00, mid-peak periods are from 7:00 to 11:00 and 17:00 to 19:00, and on-peak periods are from 11:00 to 17:00.

Without loss of generality, the rated capacity of the transformer that serves the community is assumed to be 50 kVA and it operates at 0.9 power factor lagging, which is a typical case in residential communities in North America [6]. As such, the rated real power of the transformer is set at 45 kW.

It is worth noting that the proposed system does not consider additional power system constraints, such as voltage thresholds. The reason for this is because the real-world data collected to execute the experiments originates from homes within urban areas that are typically connected to strong/stiff

TABLE 2. Nameplate Ratings of DERs Used in Simulations

DER	Nameplate (Simulated)	Nameplate (Real-World)
PV	5 kW	2 x 6 kW
BESS	6 kW, 25 kWh	-
EV	6 kW, 45 kWh	6 kW, 45 kWh
ST	0-2 kW	6 kW (E-Load)

grids, where large voltage variations are not particularly common [50].

The real-world experiment is conducted at the KCM and is executed using a PV, EV, and an electric load (E-Load) that mimics the behavior of a ST. The nameplate ratings of these DERs can be found in Table 2. The market intervals used for the experimental results are in 5-minute intervals.

A. IMPACT OF FUZZY BESS BIDDING STRATEGY ON PEAK DEMAND

The objective of the first simulated experiment is to determine the impact of the fuzzy BESS bidding strategy on the peak demand of the community. First, a baseline is established, whereby each homeowner within the 8-home community is configured to have a selfish strategy for their BESS, EV, and ST, as depicted in Figure 10. Subsequently, the strategy distribution of the BESSs is incremented by one helpful BESS at a time, with community load profiles being generated from a distribution of 8 selfish BESSs and 0 helpful BESSs, to 0 selfish BESSs and 8 helpful BESSs. This type of sensitivity analysis is useful in isolating the impact of the BESS bidding strategy on the peak demand of the community. Thus, the results of the aforementioned sensitivity analysis can be seen in Figure 11, where the peak load of the community reduces almost linearly as the number of helpful BESSs increase. The peak load reduces from 101.7 kW when there are 8 selfish BESSs, to 53.3 kW when there are 8 helpful BESSs, which is a decrease of 62%. The load profiles of the community based on these two scenarios are shown in Figure 12, where the daily peak reduction can be clearly seen when helpful BESSs are in the majority.

Furthermore, Figure 13 shows the difference in behavior of helpful BESSs and selfish BESSs as a function of their power output. As seen in the figure, the daily peak demand aligns with the coincident charging of selfish BESSs, while during the same time frame, helpful BESSs tend to discharge (negative values for power output signify that the BESS is discharging). Thus, helpful BESSs play a dominant role in reduction of peak demand for the community, and contribute a maximum cumulative reduction of 40.8 kW, which is 85% of the total reduction observed during the time of the study.

B. IMPACT OF DEMAND CAP ON PEAK DEMAND

Using the results of the previous subsection, the peak load of the community with 8 helpful BESSs is 53.3 kW, which exceeds the maximum transformer capacity of 45 kW, and would require the DSO to upgrade the transformer as a result. To avoid this upgrade, a demand cap of 45 kW is applied to the market for the entirety of the time under study to limit

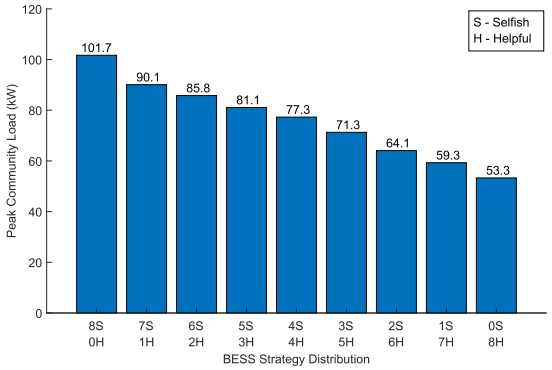

FIGURE 11. Impact of helpful BESSs on peak demand.

the allowable demand of the community. The resultant load profile of the community is shown in Figure 14, where it can be seen that the peak demand of the community reduces to 41 kW. However, applying the demand cap can result in some negative consequences, as the demand cap constrains the market and tends to drive up the MCP [51]. As a result, DERs, such as EVs, do not get the opportunity to retain their desired SoC. This is shown in Figure 15, where helpful EVs bidding in the non-demand cap market achieve 100% SoC every day, whereas EVs within the demand cap market retain a maximum of 62% SoC.

Utilizing the results of Section VI.A and Section VI.B, a financial assessment is carried out on five DSOs within Ontario, Canada, to investigate the total CAPEX saved by the proposed system as a result of its reduction of peak demand. The data for the number of existing 50 kVA transformers in their respective territories is publicly available on their websites, while the prices for 50 kVA and 125 kVA transformers are $3,172.13 and $10,570.37, respectively [52]. To support the baseline peak load of 101.7 kW as found in Section VI.A, the transformer must be upgraded to 125 kVA. On the other hand, the demand cap scenario in Section VI.B generates a peak load of 41 kW, which avoids the upgrades entirely, but the transformers would still need to be replaced at least once during their lifetime. The results of the financial assessment are generated using (13) and shown in Table 3, where an average of $102.5 M of CAPEX is saved per DSO, which is a total savings of 57.1%.

C. BENCHMARKING OF PROPOSED SYSTEM

The benchmarking of the proposed system in terms of transaction latency is performed as per the monte carlo-based methodology defined in [29]. Namely, eight client applications are launched simultaneously, which invoke the *submitBid* and *doDoubleAuction* methods of the smart contracts for 1000 iterations. The consensus mechanism used for the benchmark is pBFT. The number of nodes participating in the pBFT consensus process is varied from 2 to 12 in order to determine their effect on the overall execution time of the aforementioned functions. It is important to reiterate that the number of nodes does not equal the number of

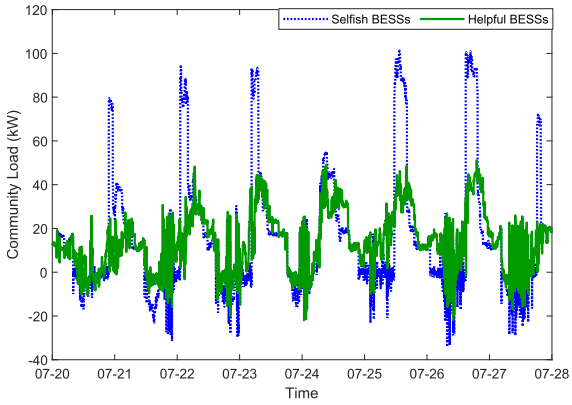

FIGURE 12. Load profile comparison of a community with either selfish or helpful BESSs.

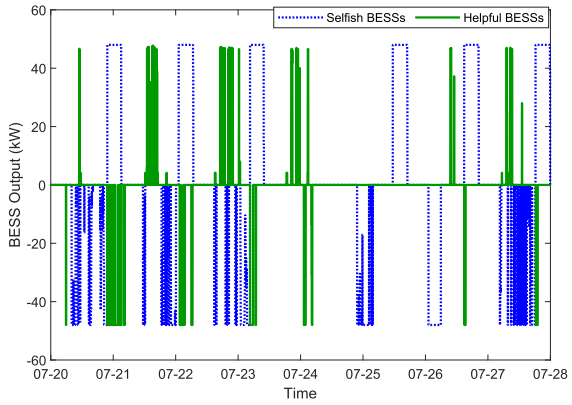

FIGURE 13. Power output of selfish and helpful BESSs.

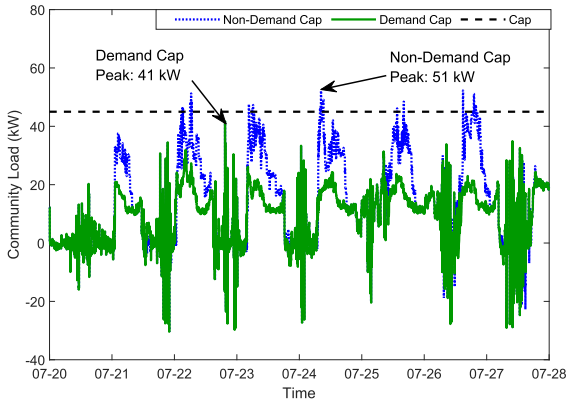

FIGURE 14. Community load profile with and without demand cap.

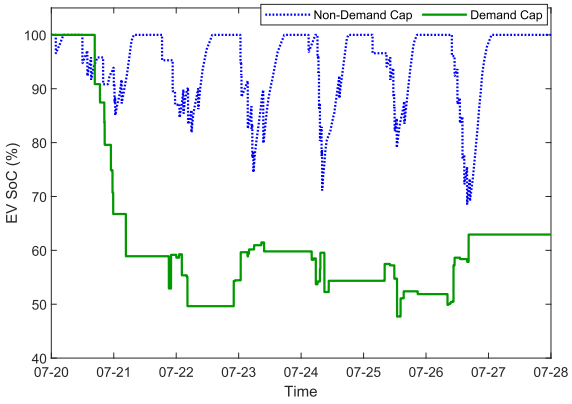

FIGURE 15. Helpful EV SoC with and without demand cap.

homeowners engaging in energy trading within the proposed system. As explained in Section II, multiple peers, or in this case, homeowners, can be assigned to a single node, and interact with the node using a client application. Thus, the number of active client applications is the true measure of the number of homeowners engaging in the trading process.

To facilitate the benchmarking of the trading process, the ledger is loaded with 1000 bids from 8 different client applications using the *submitBid* function, and the MCP is calculated for the 1000 bids for 1000 iterations using the *doDoubleAuction* function. The consensus execution time, otherwise referred to as the transaction latency, is calculated by recording the timestamp at the transaction proposal stage and subtracting it from the timestamp recorded as soon as the transaction is committed to the ledger. The benchmarking is carried out on a 2.2 GHz, 8GB RAM computer running the Ubuntu 16.04 operating system and HLF version 1.4. The block size and block speed are retained from the default settings as 10 transactions per block, and 2 seconds, respectively.

The benchmarking results can be seen in Figure 16, where the *submitBid* function has little latency differential from 2 nodes (3.62 s) to 12 nodes (5.72 s). This is in contrast to the *doDoubleAuction* function, where the latency differential almost triples from 3.5 s at 2 nodes to 11.4 s at 12 nodes. At 12 nodes, the latency of the *doDoubleAuction* function is roughly double of the *submitBid* function, which is to be expected, since the computational complexity of the former is greater than the latter. Nonetheless, even at 12 nodes, the proposed system demonstrates good scalability, where the total transaction time of both functions at 12 nodes is 17.12 s, and sufficient to execute RETS, where typical market intervals operate in the time resolution of minutes [51].

D. REAL-WORLD EXPERIMENT

The real-world experiment is executed at the KCM, which is a microgrid located in Vaughan, Canada, and equipped with four smart homes (Smart Home A, Smart Home B, Solar Hut, Wind Hut), 35 kW of PV, a Nissan Leaf EV, and an E-Load as seen in Figure 17. An aerial shot of the microgrid can be seen in Figure 18, which shows the PV system and smart homes on the west side of the microgrid. To make the microgrid more representative of a residential community, the PV is curtailed to 10 kW, while the controllable loads are considered to be the E-Load and the EV. The objective of the experiment is to demonstrate how the microgrid utilizes the proposed system to serve the E-Load and EV by the on-site PV, aiming to minimize any import from the DSO-controlled grid. The permissioned blockchain platform discussed in Section V is hosted on a Linux-based laptop, with nodes being placed on a Windows-based laptop, a NI-PXI controller, and Raspberry

TABLE 3. CAPEX Savings of Ontario DSOs

DSO	Transformer Replacements	Baseline CAPEX ($)	Demand Cap CAPEX ($)	CAPEX Savings ($)
Alectra	102,260	756.5 M	324.4 M	432.1 M
Toronto	54,081	400.1 M	171.2 M	228.5 M
Ottawa	42,348	313.3 M	134.3 M	179.0 M
London	13,535	100.1 M	42.9 M	57.2 M
Kitchener	9,583	70.9 M	30.4 M	40.5 M
Averages	**24,262**	**179.5 M**	**76.9 M**	**102.5 M**

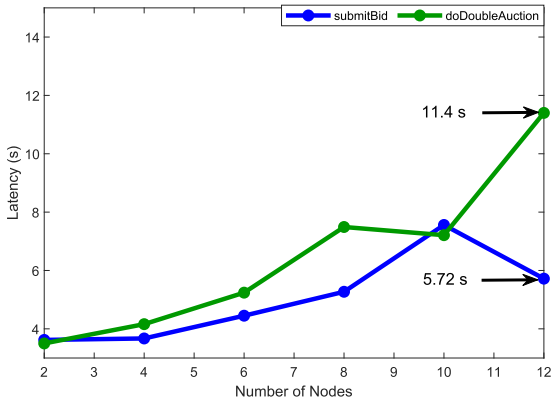

FIGURE 16. Transaction latency of proposed system.

Pi B+, respectively. Each node uses the MODBUS protocol to actuate the DERs associated with it, and uses a REST API to access functions of the smart contract [49].

A time-series graph of the experiment can be seen in Figure 19, which divides the experiment into 3 bidding rounds of 2 minutes each. In Bid #1 at 11:50:10, the E-Load bids at $0.10/5 kWh, while the PV bids at $0.05/10 kWh, with both DERs using the using the *submitBid* function of the smart contract to submit bids to the ledger. Then, the *doDoubleAuction* function is executed to determine a MCP of $0.05/kWh. The MCP is then broadcast to all the nodes, where only the E-Load is turned on as seen in Figure 19. The second round of bidding includes the EV, which outbids the previous E-Load bid at $0.15/5 kWh, resulting in an MCP of $0.10/kWh. At this point, the PV supply of 10 kW cannot support both the E-Load and EV, and this is reflected by the MCP result, which dictates that the EV is turned on, and the E-Load is turned off. Finally, in the third round of bidding, the E-Load matches the EV bid at $0.15/5 kWh, and the resultant MCP is $0.16/kWh. The MCP is equivalent to the TOU price of the DSO at the time, and thus, both the EV and the E-Load are turned on. This can be seen in Figure 19, as the individual plots for the EV and E-Load rise to approximately 6 kW, while the measurement at the point of common coupling (PCC) indicates that the microgrid imports roughly 1 kW from the DSO to satisfy the overall demand. It is worth noting that the combined total execution time of both smart contract functions across the three bidding intervals are 7.84 s, 7.76 s, and 8.18 s, which are consistent with the results obtained during the benchmarking evaluation.

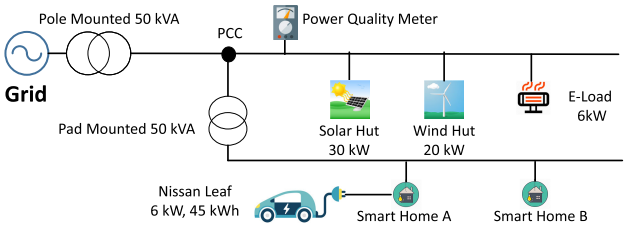

FIGURE 17. Single line diagram of Kortright Centre Microgrid.

FIGURE 18. Aerial shot of the Kortright Centre Microgrid, which shows the PV system and smart homes on the west side of the microgrid.

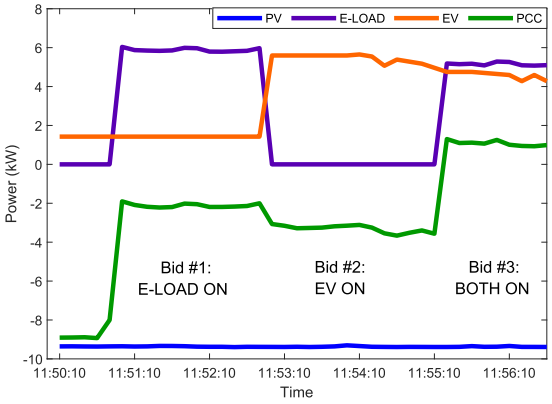

FIGURE 19. Demonstration of DERs responding to bid outcomes.

VII. CONCLUSION

This article proposed a permissioned blockchain-based RETS that enabled homeowners to trade energy and reduce peak demand. A fuzzy bidding strategy was developed for BESSs to distinguish their operation as selfish or helpful, thus enabling helpful BESSs to alter their schedule to reduce peak demand. Simulation results revealed that the proposed system reduced the peak load of the community by 62%, thus generating an average CAPEX savings of $102.5M for DSOs in Ontario. The proposed system was deployed at a Canadian microgrid using the HLF platform, and used to demonstrate how the microgrid could reduce demand and minimize energy imports from the DSO. The execution time of the proposed smart contract was benchmarked at 17.12 s, which is sufficient for RETS. The future scope of the work includes extending the proposed system to accommodate trading between communities to further reduce the peak demand of an entire territory. Furthermore, the monetary

incentive for homeowners to participate in demand response events will also be quantified as a function of CAPEX savings of the DSO.

REFERENCES

[1] M. V. Kirthiga, S. A. Daniel, and S. Gurunathan, "A methodology for transforming an existing distribution network into a sustainable autonomous micro-grid," *IEEE Trans. Sustain. Energy*, vol. 4, no. 1, pp. 31–41, Jan. 2013.

[2] W. Tushar, T. K. Saha, C. Yuen, D. Smith, and H. V. Poor, "Peer-to-peer trading in electricity networks: An overview," *IEEE Trans. Smart Grid*, vol. 11, no. 4, pp. 3185–3200, Jul. 2020.

[3] S. V. Akram, P. K. Malik, R. Singh, G. Anita, and S. Tanwar, "Adoption of blockchain technology in various realms: Opportunities and challenges," *Secur. Privacy*, vol. 3, no. 5, pp. 109–125, Apr. 2020.

[4] J. Han, C.-S. Choi, W.-K. Park, I. Lee, and S.-H. Kim, "Smart home energy management system including renewable energy based on ZigBee and PLC," *IEEE Trans. Consum. Electron.*, vol. 60, no. 2, pp. 198–202, May 2014.

[5] U. Zafar, S. Bayhan, and A. Sanfilippo, "Home energy management system concepts, configurations, and technologies for the smart grid," *IEEE Access*, vol. 8, pp. 119271–119286, Jun. 2020.

[6] M. K. Gray and W. G. Morsi, "On the role of prosumers owning rooftop solar photovoltaic in reducing the impact on transformer's aging due to plug-in electric vehicles charging," *Electr. Power Syst. Res.*, vol. 143, pp. 563–572, Feb. 2017.

[7] S. Saxena, H. Farag, A. Brookson, H. Turesson, and H. Kim, "Design and field implementation of blockchain based renewable energy trading in residential communities," in *Proc. 2nd Int. Conf. Smart Grid Renew. Energy (SGRE)*, Nov. 2019, pp. 1–6.

[8] K. Anoh, S. Maharjan, A. Ikpehai, Y. Zhang, and B. Adebisi, "Energy peer-to-peer trading in virtual microgrids in smart grids: A game-theoretic approach," *IEEE Trans. Smart Grid*, vol. 11, no. 2, pp. 1264–1275, Mar. 2020.

[9] Z. Li, J. Kang, R. Yu, D. Ye, Q. Deng, and Y. Zhang, "Consortium blockchain for secure energy trading in industrial Internet of Things," *IEEE Trans. Ind. Informat.*, vol. 14, no. 8, pp. 3690–3700, Aug. 2018.

[10] N. Z. Aitzhan and D. Svetinovic, "Security and privacy in decentralized energy trading through multi-signatures, blockchain and anonymous messaging streams," *IEEE Trans. Depend. Sec. Comput.*, vol. 15, no. 5, pp. 840–852, Sep. 2018.

[11] Y. Xiao, N. Zhang, W. Lou, and Y. T. Hou, "A survey of distributed consensus protocols for blockchain networks," *IEEE Commun. Surveys Tuts.*, vol. 22, no. 2, pp. 1432–1465, 2nd Quart., 2020.

[12] Z. Su, Y. Wang, Q. Xu, M. Fei, Y.-C. Tian, and N. Zhang, "A secure charging scheme for electric vehicles with smart communities in energy blockchain," *IEEE Internet Things J.*, vol. 6, no. 3, pp. 4601–4613, Jun. 2019.

[13] J. Kang, R. Yu, X. Huang, S. Maharjan, Y. Zhang, and E. Hossain, "Enabling localized peer-to-peer electricity trading among plug-in hybrid electric vehicles using consortium blockchains," *IEEE Trans. Ind. Informat.*, vol. 13, no. 6, pp. 3154–3164, Dec. 2017.

[14] R. Khalid, N. Javaid, A. Almogren, M. U. Javed, S. Javaid, and M. Zuair, "A blockchain-based load balancing in decentralized hybrid P2P energy trading market in smart grid," *IEEE Access*, vol. 8, pp. 47047–47062, Mar. 2020.

[15] A. Yahaya, N. Javaid, F. Alzahrani, A. Rehman, I. Ullah, A. Shahid, and M. Shafiq, "Blockchain based sustainable local energy trading considering home energy management and demurrage mechanism," *Sustainability*, vol. 12, no. 8, pp. 3385–3412, Apr. 2020.

[16] W. Hou, L. Guo, and Z. Ning, "Local electricity storage for blockchain-based energy trading in industrial Internet of Things," *IEEE Trans. Ind. Informat.*, vol. 15, no. 6, pp. 3610–3619, Jun. 2019.

[17] J. Guerrero, A. C. Chapman, and G. Verbic, "Decentralized P2P energy trading under network constraints in a low-voltage network," *IEEE Trans. Smart Grid*, vol. 10, no. 5, pp. 5163–5173, Sep. 2019.

[18] F. Luo, Z. Y. Dong, G. Liang, J. Murata, and Z. Xu, "A distributed electricity trading system in active distribution networks based on multi-agent coalition and blockchain," *IEEE Trans. Power Syst.*, vol. 34, no. 5, pp. 4097–4108, Sep. 2019.

[19] M. Afzal, Q. Huang, W. Amin, K. Umer, A. Raza, and M. Naeem, "Blockchain enabled distributed demand side management in community energy system with smart homes," *IEEE Access*, vol. 8, pp. 37428–37439, Feb. 2020.

[20] S. Seven, G. Yao, A. Soran, A. Onen, and S. M. Muyeen, "Peer-to-peer energy trading in virtual power plant based on blockchain smart contracts," *IEEE Access*, vol. 8, pp. 175713–175726, Sep. 2020.

[21] M. O. Okoye, J. Yang, J. Cui, Z. Lei, J. Yuan, H. Wang, H. Ji, J. Feng, and C. Ezeh, "A blockchain-enhanced transaction model for microgrid energy trading," *IEEE Access*, vol. 8, pp. 143777–143786, Jul. 2020.

[22] M. Li, D. Hu, C. Lal, M. Conti, and Z. Zhang, "Blockchain-enabled secure energy trading with verifiable fairness in industrial Internet of Things," *IEEE Trans. Ind. Informat.*, vol. 16, no. 10, pp. 6564–6574, Oct. 2020.

[23] A. Kumari, R. Gupta, S. Tanwar, S. Tyagi, and N. Kumar, "When blockchain meets smart grid: Secure energy trading in demand response management," *IEEE Netw.*, vol. 34, no. 5, pp. 299–305, Sep. 2020.

[24] A. Kumari, A. Shukla, R. Gupta, S. Tanwar, S. Tyagi, and N. Kumar, "ET-DeaL: A P2P smart contract-based secure energy trading scheme for smart grid systems," in *Proc. IEEE Conf. Comput. Commun. Workshops (INFOCOM WKSHPS)*, Jul. 2020, pp. 1051–1056.

[25] S. Tanwar, S. Kaneriya, N. Kumar, and S. Zeadally, "ElectroBlocks: A blockchain-based energy trading scheme for smart grid systems," *Int. J. Commun. Syst.*, vol. 33, no. 15, pp. 1–15, Jun. 2020.

[26] P. Singh, A. Nayyar, A. Kaur, and U. Ghosh, "Blockchain and fog based architecture for Internet of everything in smart cities," *Future Internet*, vol. 12, no. 4, pp. 1–12, Mar. 2020.

[27] T. Morstyn and M. D. McCulloch, "Multiclass energy management for peer-to-peer energy trading driven by prosumer preferences," *IEEE Trans. Power Syst.*, vol. 34, no. 5, pp. 4005–4014, Sep. 2019.

[28] Y. Wang, Z. Su, and N. Zhang, "BSIS: Blockchain-based secure incentive scheme for energy delivery in vehicular energy network," *IEEE Trans. Ind. Informat.*, vol. 15, no. 6, pp. 3620–3631, Jun. 2019.

[29] T. T. A. Dinh, J. Wang, G. Chen, R. Liu, B. C. Ooi, and K.-L. Tan, "BLOCKBENCH: A framework for analyzing private blockchains," in *Proc. ACM Int. Conf. Manage. Data*, May 2017, pp. 1085–1100.

[30] M. Andoni, V. Robu, D. Flynn, S. Abram, D. Geach, D. Jenkins, P. McCallum, and A. Peacock, "Blockchain technology in the energy sector: A systematic review of challenges and opportunities," *Renew. Sustain. Energy Rev.*, vol. 100, pp. 143–174, Feb. 2019.

[31] Z. Zheng, S. Xie, H. Dai, X. Chen, and H. Wang, "An overview of blockchain technology: Architecture, consensus, and future trends," in *Proc. IEEE Int. Congr. Big Data (BigData Congr.)*, Jun. 2017, pp. 557–564.

[32] M. Belotti, N. Bozic, G. Pujolle, and S. Secci, "A vademecum on blockchain technologies: When, which, and how," *IEEE Commun. Surveys Tuts.*, vol. 21, no. 4, pp. 3796–3838, 4th Quart., 2019.

[33] J. Liu and Z. Liu, "A survey on security verification of blockchain smart contracts," *IEEE Access*, vol. 7, pp. 77894–77904, Jun. 2019.

[34] R. Guo, H. Shi, Q. Zhao, and D. Zheng, "Secure attribute-based signature scheme with multiple authorities for blockchain in electronic health records systems," *IEEE Access*, vol. 6, pp. 11676–11686, Feb. 2018.

[35] A. Kaur, A. Nayyar, and P. Singh, "Blockchain: A path to the future," in *Cryptocurrencies and Blockchain Technology Applications*. Hoboken, NJ, USA: Wiley, 2020, ch. 2, pp. 25–42.

[36] A. Jabbar and S. Dani, "Investigating the link between transaction and computational costs in a blockchain environment," *Int. J. Prod. Res.*, vol. 58, no. 11, pp. 3423–3436, Apr. 2020.

[37] W. Tushar, T. K. Saha, C. Yuen, T. Morstyn, Nahid-Al-Masood, H. V. Poor, and R. Bean, "Grid influenced Peer-to-Peer energy trading," *IEEE Trans. Smart Grid*, vol. 11, no. 2, pp. 1407–1418, Mar. 2020.

[38] K. Mahmud, M. J. Hossain, and G. E. Town, "Peak-load reduction by coordinated response of photovoltaics, battery storage, and electric vehicles," *IEEE Access*, vol. 6, pp. 29353–29365, 2018.

[39] P. H. Divshali, B. J. Choi, and H. Liang, "Multi-agent transactive energy management system considering high levels of renewable energy source and electric vehicles," *IET Gener., Transmiss. Distrib.*, vol. 11, no. 15, pp. 3713–3721, Oct. 2017.

[40] C. Jiang, R. Torquato, D. Salles, and W. Xu, "Method to assess the power-quality impact of plug-in electric vehicles," *IEEE Trans. Power Del.*, vol. 29, no. 2, pp. 958–965, Apr. 2014.

[41] J. W. Smith, R. Dugan, and W. Sunderman, "Distribution modeling and analysis of high penetration PV," in *Proc. IEEE Power Energy Soc. Gen. Meeting*, Jul. 2011, pp. 1–7.

[42] P. Hietaharju, M. Ruusunen, and K. Leiviskä, "A dynamic model for indoor temperature prediction in buildings," *Energies*, vol. 11, no. 6, pp. 1477–1497, Jun. 2018.
[43] Y. Li, Z. Yan, S. Chen, X. Xu, and C. Kang, "Operation strategy of smart thermostats that self-learn user preferences," *IEEE Trans. Smart Grid*, vol. 10, no. 5, pp. 5770–5780, Sep. 2019.
[44] J. Nicolaisen, V. Petrov, and L. Tesfatsion, "Market power and efficiency in a computational electricity market with discriminatory double-auction pricing," *IEEE Trans. Evol. Comput.*, vol. 5, no. 5, pp. 504–523, Oct. 2001.
[45] B. Sütterlin, T. A. Brunner, and M. Siegrist, "Who puts the most energy into energy conservation? A segmentation of energy consumers based on energy-related behavioral characteristics," *Energy Policy*, vol. 39, no. 12, pp. 8137–8152, Dec. 2011.
[46] M. N. Faqiry and S. Das, "Double-sided energy auction in microgrid: Equilibrium under price anticipation," *IEEE Access*, vol. 4, pp. 3794–3805, Jul. 2016.
[47] V. Venizelou, G. Makrides, V. Efthymiou, and G. E. Georghiou, "Residential consumption responsiveness under time-varying pricing," in *Proc. IEEE Int. Energy Conf. (ENERGYCON)*, Jun. 2018, pp. 1–6.
[48] C.-H. Yoo, I.-Y. Chung, H.-J. Lee, and S.-S. Hong, "Intelligent control of battery energy storage for multi-agent based microgrid energy management," *Energies*, vol. 6, no. 10, pp. 4956–4979, Sep. 2013.
[49] C. Ma, X. Kong, Q. Lan, and Z. Zhou, "The privacy protection mechanism of hyperledger fabric and its application in supply chain finance," *Cybersecurity*, vol. 2, no. 1, pp. 1–9, Jan. 2019.
[50] A. S. Subburaj and S. B. Bayne, "Battery and wind system in weak/strong grid analysis," in *Proc. IEEE Ind. Appl. Soc. Annu. Meeting*, Oct. 2015, pp. 1–6.
[51] J. C. Fuller, K. P. Schneider, and D. Chassin, "Analysis of residential demand response and double-auction markets," in *Proc. IEEE Power Energy Soc. Gen. Meeting*, Jul. 2011, pp. 1–7.
[52] Larson Electronics. (Jan. 2020). *Cost of Transformers*. Accessed: Jan. 2020. [Online]. Available: https://www.larsonelectronics.com/category/719/100-112-5-kva-industrial-transformers

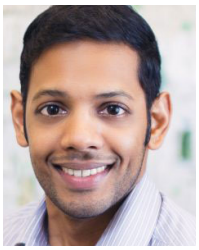

SHIVAM SAXENA (Student Member, IEEE) received the M.A.Sc. degree in computer engineering from the Electrical Engineering and Computer Science Department, Lassonde School of Engineering, York University, Toronto, Canada, where he is currently pursuing the Ph.D. degree. His current research interests include designing and deploying distributed control and communication frameworks within power distribution systems, with an active focus on evaluating the feasibility of technologies such as Internet of Things and Blockchain technology. He is also a licensed professional engineer in (P.Eng.) in the province of Ontario, Canada.

HANY E. Z. FARAG (Senior Member, IEEE) received the B.Sc. (Hons.) and M.Sc. degrees in electrical engineering from Assiut University, Assiut, Egypt, in 2004 and 2007, respectively, and the Ph.D. degree in electrical and computer engineering from the University of Waterloo, in 2013. Since July 2013, he has been with the Department of Electrical Engineering and Computer Science, Lassonde School of Engineering, York University, where he is currently an Associate Professor. His current research interests include power distribution networks, the integration of distributed and renewable energy resources, electric mobility, modeling, analysis, and design of microgrids, applications of multi-agent, and blockchain technologies in smart grids. He is a Registered Professional Engineer in Ontario.

AIDAN BROOKSON received the master's degree in mechanical engineering and the M.A.Sc. degree from Ryerson University, with his thesis focusing on renewable energy and energy storage system applications for residential buildings and communities. He has conducted numerous technical evaluations and research projects involving solar photovoltaics, heat pumps, and energy storage systems. He is currently serving as the Research Director for Volta Research, a not-for-profit organization dedicated to the advancement and deployment of low carbon technologies.

HJALMAR TURESSON received the B.Sc. degree in biology from Lund University, Sweden, the M.Sc. degree in neural and behavioral sciences from the University of Tubingen, Germany, and the Ph.D. degree in neuro-science from Princeton University, USA. He is currently a Postdoctoral Fellow with the Schulich School of Business, York University, Canada.

HENRY KIM is currently an Associate Professor with the Schulich School of Business, York University, Toronto, Canada. He is also the Director of the Blockchain Lab, which has engaged in projects with the UN, Ontario Ministry of Agriculture, Toronto and Region Conservation Authority, and the Tapscott Blockchain Research Institute.